Dispersion of the prehistory distribution for non-gradient systems

Jinjie Zhu[1], Jiong Wang[1], Shang Gao[1] and Xianbin Liu[2]

[1] School of Mechanical Engineering, Nanjing University of Science and Technology, Nanjing 210094, People's Republic of China
[2] State Key Laboratory of Mechanics and Control of Mechanical Structures, College of Aerospace Engineering, Nanjing University of Aeronautics and Astronautics, Nanjing 210016, People's Republic of China
E-mail: zhujinjie95@njust.edu.cn

Abstract. The most probable escape path can reveal the optimal fluctuation with overwhelming probability for vanishing noise during escape. However, it fails to offer information for the feature of the nearby paths, while the dispersion of the prehistory distribution does. For gradient systems, the dispersion can be obtained via a relaxation method which takes the advantage of the time reversibility of the fluctuation-dissipation relation. For non-gradient systems, due to the breaking of the time-reversal symmetry, the traditional relaxation method cannot be applied. In this paper, we investigate the dispersion of the exit phenomena in the Maier–Stein system for three sets of parameters. For the gradient case, the traditional relaxation method is extended to the 2D situation. For the non-gradient case, we propose a revised version of the relaxation method which relies on the computation of quasipotential. The results are compared with those of Monte Carlo simulation which shows the efficiency of the algorithms.

Contents

1. Introduction

Stochasticity is an essential feature of nature, wherein noise could play a nontrivial role, e.g. the cultural evolution of vocalizations in animals [1], the expression of the spatiotemporal patterns in brains [2], rumor spreading in complex social networks [3] and population fitness [4]. For dynamical systems, noise has surprised the researchers by its constructive functions. Among them, stochastic resonance [5] and coherence resonance [6] have been investigated extensively in theory and experiments.

Considering the long-term behaviors of dynamical systems, noise could drive the state to an arbitrary range away from its initial stationary position even if the noise strength approaches zero. This phenomenon has been investigated in the framework of the large deviation theory [7], which opens up a new perspective on the stochastic dynamical behaviors of noise-perturbed systems. The core of this theory is the action functional defined by Freidlin and Wentzell. The path with the least value of the action functional renders the most probable escape path (MPEP) or the minimum action path (MAP) or the optimal path, which is the path with overwhelming probability over other exit paths for vanishing noise. The MPEP can reveal the details of stochastic transitions out of oscillatory states as is investigated by Cruz *et al* in biochemical reactions [8], capture the wave-number selection in nonequilibrium systems [9] and show the competence behavior in *B. subtilis* under the influence of stable Lévy noise [10], etc. Due to the importance of the MPEP, numerous methods have been proposed, such as the geometric minimum action method (gMAM) [11], action plot method [12], ordered upwind method (OUM) and its improved versions [13–16].

The MPEP captures the most probable exit behavior for vanishing noise while fails to uncover the nearby fluctuational feature for finite noise. The prehistory probability

distribution [17] provides a way of observing nearby fluctuational paths around the MPEP. The dispersion of the prehistory problem reflects the sensitivity of the fluctuation along the MPEP, showing a relative width of the 'WKB tube' [18]. Traditional Monte Carlo simulation takes exponentially large time for obtaining the escape paths for small noise, which is revealed by computing the mean first passage time. Fortunately, for gradient systems, the MPEP follows the time-reversed path of the relaxation [17]. Therefore, Morillo *et al* proposed a relaxation method for 1D gradient system [19, 20]. This method starts the initial point from the end point of the exit process and let it evolve along the relaxational path. However, for non-gradient systems, due to the lack of detailed balance, the time-reversal symmetry of the fluctuation-dissipation relation will be broken [21, 22], which results in the failure of the relaxation method.

In this paper, we investigate the dispersion of the prehistory distribution for the Maier–Stein system. It is a well-studied model which describes noise-induced escape of a particle from a metastable state in a non-linear field. Three sets of parameters are considered for both gradient and non-gradient cases. For the gradient case, the relaxation method proposed by Morillo *et al* is verified for 2D situation. For the non-gradient case, we proposed a revised relaxation method. The results by these methods are compared with those of the Monte Carlo simulations.

2. Maier–Stein model

To investigate the dispersion of the prehistory distribution, the well-known Maier–Stein system is applied. This model is proposed by Maier and Stein [23–27] to study the exit phenomena for systems lacking detailed balance, which goes:

$$
\begin{aligned}
\dot{x} &= x - x^3 - \alpha x y^2 + \xi_1(t), \\
\dot{y} &= -\mu(1 + x^2)y + \xi_2(t) \\
\langle \xi_i(t) \rangle &= 0, \langle \xi_i(t)\xi_j(t-\tau) \rangle = D\delta_{ij}\delta(\tau)
\end{aligned}
\tag{1}
$$

where α and μ are parameters and D is the strength of the noise. For the deterministic version of the system, there are three equilibrium points: $(\pm 1, 0)$ and $(0, 0)$ regardless of the choice for the parameters. The first two are stable and the origin is an unstable saddle point. The vector field is a classic double-well model which is gradient if and only if $\alpha = \mu$ [28]. Figure 1 illustrates the potential landscape for $\alpha = \mu = 1$. It can be seen from figure 1 that the potential energy is symmetric along the x-axis and y-axis. The symmetry will have some impacts on the exit phenomena, as we will see later. For $\alpha \neq \mu$, the condition of detailed balance will be broken which means the time-reversibility of the fluctuational and relaxational paths does not hold anymore.

Before we uncover the characteristics of the dispersion for the exit process, the fluctuational paths and MPEPs will be discussed briefly.

Freidlin and Wentzell defined the following action functional [7]:

$$
S(\varphi) = \int_{t_0}^{t_f} L(\dot{\boldsymbol{x}}, \boldsymbol{x}) \mathrm{d}t = \int_{t_0}^{t_f} \frac{1}{2}(\dot{\boldsymbol{x}} - \boldsymbol{F}(\boldsymbol{x}))^T (\dot{\boldsymbol{x}} - \boldsymbol{F}(\boldsymbol{x})) \mathrm{d}t = \frac{1}{2} \int_{t_0}^{t_f} \boldsymbol{\lambda}^T \boldsymbol{\lambda} \mathrm{d}t
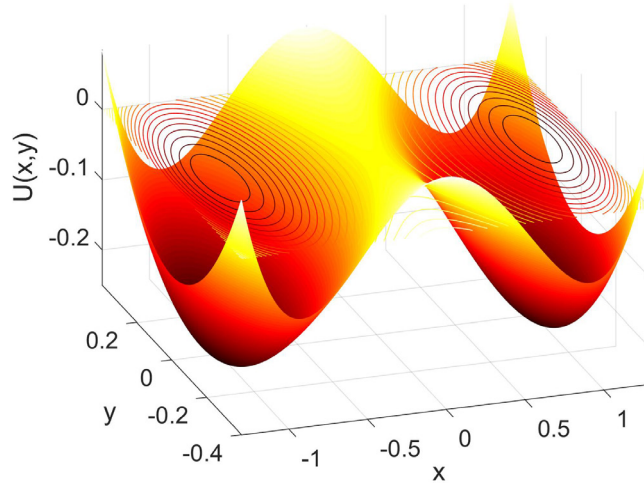\tag{2}
$$

Figure 1. Landscape of the potential energy of system (1). Parameters are: $\alpha = \mu = 1$. The representative potential can be readily computed as $U(x, y) = -\left(x^2 - y^2 - x^4/2 - x^2y^2\right)/2$.

where $L\left(\dot{\boldsymbol{x}}, \boldsymbol{x}\right)$ is the Lagrangian in classical mechanics, which is the Legendre transformation of the Hamiltonian. The variable $\boldsymbol{\lambda} = \dot{\boldsymbol{x}} - \boldsymbol{F}\left(\boldsymbol{x}\right)$ are momenta which represent the action of noise during the fluctuation process. The path corresponding to the minimal value of the action functional renders the MPEP. The fluctuational paths satisfy the following auxiliary Hamiltonian system [12]:

$$
\begin{aligned}
\dot{\boldsymbol{x}} &= \begin{bmatrix} \dot{x} \\ \dot{y} \end{bmatrix} = \boldsymbol{F}\left(\boldsymbol{x}\right) + \boldsymbol{\lambda} = \begin{bmatrix} x - x^3 - \alpha x y^2 \\ -\mu\left(1 + x^2\right)y \end{bmatrix} + \begin{bmatrix} \lambda_1 \\ \lambda_2 \end{bmatrix}, \\
\dot{\boldsymbol{\lambda}} &= \begin{bmatrix} \dot{\lambda}_1 \\ \dot{\lambda}_2 \end{bmatrix} = -\left[\frac{\partial \boldsymbol{F}}{\partial \boldsymbol{x}}\right]^T \boldsymbol{\lambda} = \begin{bmatrix} \left(\alpha y^2 + 3x^2 - 1\right)\lambda_1 + 2\mu x y \lambda_2 \\ 2\alpha x y \lambda_1 + \mu\left(1 + x^2\right)\lambda_2 \end{bmatrix}.
\end{aligned}
\tag{3}
$$

We choose three sets of parameters: (1) $\alpha = \mu = 1$; (2) $\alpha = 6.67, \mu = 2$; (3) $\alpha = 6.67, \mu = 1$. The fluctuational paths and MPEPs for these parameters are shown in figure 2. To compare the fluctuation behavior for them, the initial conditions are set the same as in figure 2(d). For parameter set (1), which satisfies the condition of detailed balance, the fluctuational paths in figure 2(a) also exhibit the relaxational paths back to the equilibrium point (1, 0). The MPEP is the straight line which connects (1, 0) and (0, 0). For $\alpha = 6.67, \mu = 2$, the MPEP is the same as the previous parameter sets where the symmetry remains unbroken. However, the feature of the fluctuational paths changes dramatically. The inset of figure 2(b) shows the local behavior of the fluctuation near the stable point (1, 0). For the last case, the Lagrangian manifold exhibits the topological singularity [27, 29] which is displayed by the intersection of the fluctuational paths. The MPEP bifurcates into two curves symmetric along the x-axis.

In the following, the dispersion of the prehistory distribution along the exit process will be studied for the three cases discussed above.
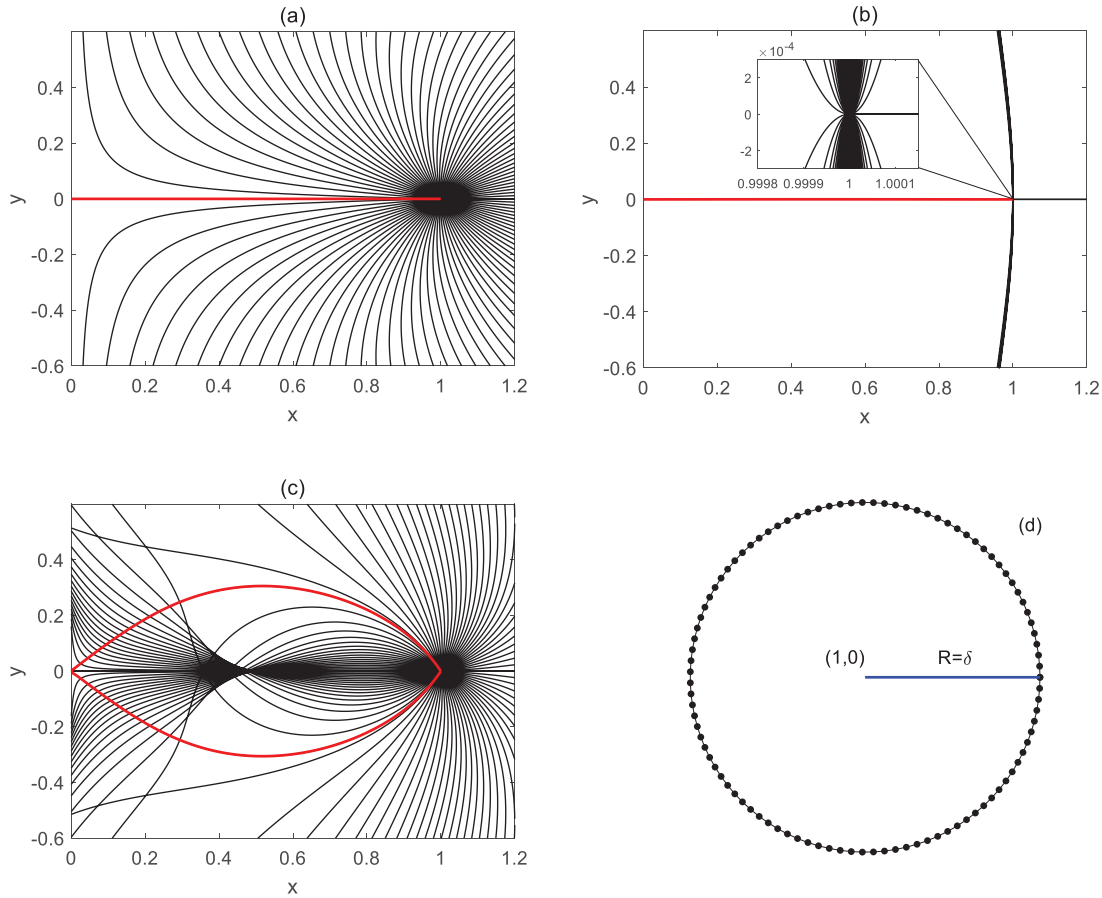
Figure 2. Optimal fluctuational paths (thin black lines) and MPEPs (thick red lines) for the Maier–Stein system with different parameters. (a) $\alpha = \mu = 1$; (b) $\alpha = 6.67, \mu = 2$; (c)$\alpha = 6.67, \mu = 1$; (d) 100 black dots distributed equally on the circle ($R = \delta = 10^{-6}$) represent the initial conditions for fluctuational paths.

3. Results

3.1. Case $\alpha = \mu = 1$

In this case, the dispersion can be investigated similarly as the relaxation method proposed by Morillo *et al* applied in 1D Langevin equation [19, 20]. It is realized by starting from the end point $\boldsymbol{x}_f$, and letting it evolve back to the initial position. The dispersion can be readily computed along the relaxational paths. To verify the efficiency of this method in our 2D case. Monte Carlo simulation results will be compared with those of the relaxation method. The prehistory distribution near the MPEP is approximately Gaussian for weak noise [17]:

$$p_h\left(\boldsymbol{x}, t; \boldsymbol{x}_f, 0\right) = \left[\frac{1}{2\pi|\boldsymbol{\Sigma}|^{1/2}}\right] \exp\left\{-\frac{1}{2}[\boldsymbol{x} - \boldsymbol{x}_{\mathrm{opt}}\left(t; \boldsymbol{x}_f\right)]^{\mathrm{T}} \boldsymbol{\Sigma}^{-1}\left[\boldsymbol{x} - \boldsymbol{x}_{\mathrm{opt}}\left(t; \boldsymbol{x}_f\right)\right]\right\} \qquad (4)$$

where $p_h\left(\boldsymbol{x}, t; \boldsymbol{x}_f, 0\right)$ denotes the prehistory distribution at time t for the given final point $\boldsymbol{x}_f$. The subscript opt represents the optimal path or the MPEP. And $\boldsymbol{\Sigma}$ is the covariance matrix for the noise. Because of the independence of the isotropic noise in

system (1), the covariance matrix $\boldsymbol{\Sigma}$ is diagonal. So the marginal distribution can be readily obtained as:

$$p_h\left(u, t; \boldsymbol{x}_f, 0\right) = \left[2\pi D\sigma_u\left(t; \boldsymbol{x}_f\right)\right]^{-\frac{1}{2}} \exp\left\{-\frac{\left[u - u_{\mathrm{opt}}\left(t; \boldsymbol{x}_f\right)\right]^2}{2D\sigma_u\left(t; \boldsymbol{x}_f\right)}\right\} \tag{5}$$

where $u = x$ or y. The dispersion of the prehistory distribution $p_h\left(u, t; \boldsymbol{x}_f, 0\right)$ is characterized by the value of $\sigma_u\left(t; \boldsymbol{x}_f\right)$. The dispersion can be further expressed as:

$$\begin{cases} \sigma_x\left(t; \boldsymbol{x}_f\right) \equiv \tilde{\sigma}_x\left(\boldsymbol{x}_{\mathrm{opt}}\left(t; \boldsymbol{x}_f\right); \boldsymbol{x}_f\right) = \tilde{\sigma}_x\left(x; \boldsymbol{x}_f\right) \\ \sigma_y\left(t; \boldsymbol{x}_f\right) \equiv \tilde{\sigma}_y\left(\boldsymbol{x}_{\mathrm{opt}}\left(t; \boldsymbol{x}_f\right); \boldsymbol{x}_f\right) = \tilde{\sigma}_y\left(x; \boldsymbol{x}_f\right) \end{cases} . \tag{6}$$

To simplify the notation, we will use $\sigma_x\left(x; \boldsymbol{x}_f\right)$ and $\sigma_y\left(x; \boldsymbol{x}_f\right)$ to represent the right hand side of equation (6) throughout this paper without further clarification. The results of the dispersion of the prehistory distribution along the MPEP are shown in figure 3 (noise strength $D = 0.1$). The non-monotonic behavior of the dispersion $\sigma_x\left(x; \boldsymbol{x}_f\right)$ or $\sigma_y\left(x; \boldsymbol{x}_f\right)$ can be observed which is consistent with the results of the 1D situation. The results of the Monte Carlo simulation show relatively good agreements with the results of the relaxation method. The mismatches, e.g. the peak in figure 3(a), are caused by the finite noise strength.

For small enough noise strength, the fluctuations or escapes to a certain position become extremely rare, which is determined by the mean first passage time. Traditional Monte Carlo simulation becomes hopeless. With the relaxation method, we can still investigate the dispersion of the exit process without waiting for the realization of the real exit path as the traditional Monte Carlo simulation.

The dispersions for different final positions by the relaxation method are illustrated in figure 4. As we can see from figures 4(a) and (c), with the final position approaching the saddle point, the dispersion $\sigma_x\left(x; \boldsymbol{x}_f\right)$ explodes, while the initial dispersion keeps constant as $1/4$. This can be explained by the calculation of the extremal position of the dispersion $\sigma_x\left(x; \boldsymbol{x}_f\right)$. Because of the independence of the dispersions $\sigma_x\left(x; \boldsymbol{x}_f\right)$ and $\sigma_y\left(x; \boldsymbol{x}_f\right)$, the extremal value of the dispersion $\sigma_u\left(x; \boldsymbol{x}_f\right)$ can be obtained by solving the following equation [19, 20]:

$$\sigma_u\left(x; \boldsymbol{x}_f\right) = \frac{1}{2U_u''\left(x, y\right)} \tag{7}$$

where $u = x$ or y. For $\sigma_x\left(x; \boldsymbol{x}_f\right)$, variable y will be considered constant. Thus, by substituting the potential energy $U(x, y)$ into equation (7), we have:

$$\sigma_x\left(x; \boldsymbol{x}_f\right) = \frac{1}{2U_x''\left(x, y\right)} = \frac{1}{2\left(3x^2 - 1 - y^2\right)} \approx \frac{1}{6x^2 - 2} \tag{8}$$

where we have used the fact $y \ll x$ along the MPEP away from the saddle point $(0, 0)$. The extremal curve is illustrated in figures 4(a) and (c) as the black dashed line, which shows the tendency of the left shift of the maximal position of $\sigma_x\left(x; \boldsymbol{x}_f\right)$ and also the explosion of it when $\boldsymbol{x}_f$ approaches the saddle.

The dispersion $\sigma_y\left(x; \boldsymbol{x}_f\right)$ is shown in figures 4(b) and (d). It can be seen that $\sigma_y\left(x; \boldsymbol{x}_f\right)$ does not explode as $\sigma_x\left(x; \boldsymbol{x}_f\right)$. The extremal position can be similarly obtained as:
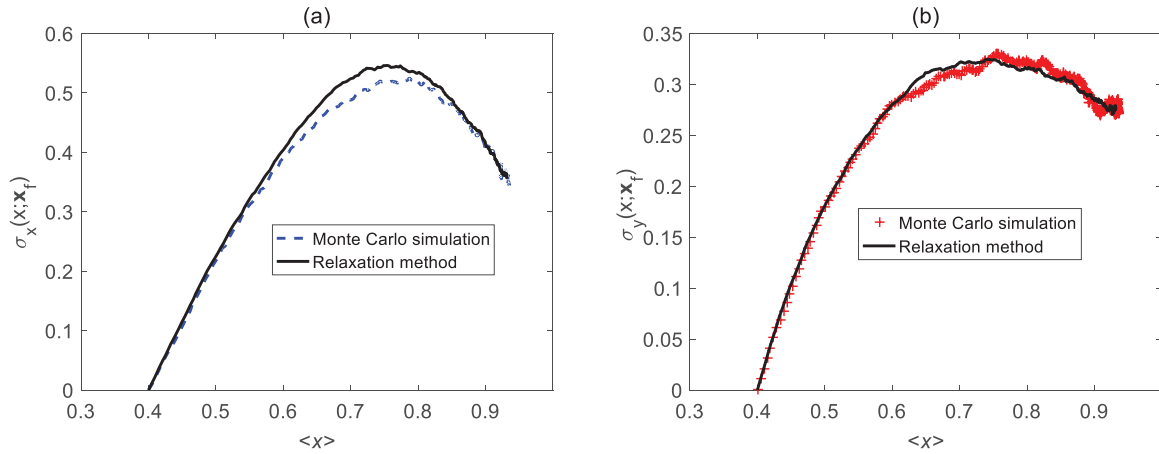
Figure 3. Dispersion of the prehistory distribution along the MPEP. (a) Dispersion along the x-axis $\sigma_x\left(x;\boldsymbol{x}_f\right)$; (b) dispersion along the y-axis $\sigma_y\left(x;\boldsymbol{x}_f\right)$. The black line represents the result by the relaxation method and the blue dashed line and the red pluses are the results of the Monte Carlo simulation. The final point $\boldsymbol{x}_f$ is set as (0.4, 0). Noise strength $D = 0.1$.

$$\sigma_y\left(x;\boldsymbol{x}_f\right) = \frac{1}{2U''_y\left(x,y\right)} = \frac{1}{2+2x^2} \tag{9}$$

which accurately predicts the initial dispersion $\sigma_y\left(x=1;\boldsymbol{x}_f\right)=1/4$. The maximal position gradually shifts left as $\boldsymbol{x}_f$ approaches the saddle. Figure 4(d) shows a dramatic decrease which is a direct result of the choice of the final position. If we choose $x=0$ as the exit boundary, the exit location distribution will be a Gaussian distribution [30]:

$$p\left(y\right) = \left(\frac{\mu}{\pi D}\right)^{1/2}\exp\left(-\frac{\mu y^2}{D}\right) \tag{10}$$

So $\sigma_y\left(x=0;\boldsymbol{x}_f=0\right) = 1/\left(2\mu\right) = 0.5$, which is consistent with our result.

3.2. Case $\alpha = 6.67$ $\mu = 2$

In this case, the MPEP remains the straight line along the x-axis. However, due to $\alpha \neq \mu$, despite that the MPEP follows the time reversed path of the relaxation process, the nearby optimal fluctuational paths do not obey the time reversibility [see figure 2(b)]. As has been discussed previously, for small noise, direct Monte Carlo simulations will take considerable large time for obtaining even one realization of an exit sample. Inspired by the relaxation method for gradient systems which satisfies the condition of detailed balance, we hope to find a similar relaxation method for non-gradient system.

3.2.1. VG relaxation method. Recall that the reason for the efficiency of the relaxation method in gradient systems is ensured by the reversed vector field for the MPEP in contrast to the original system. Specifically, if the original gradient system yields $\dot{x} = -\nabla U\left(x\right)$, the vector field for the MPEP will be $\dot{x}_{\text{opt}} = \nabla U\left(x_{\text{opt}}\right)$. For non-gradient systems, the vector field for the MPEP no longer satisfies the reversibility of the original one. As the vector field admits the decomposition [7]:
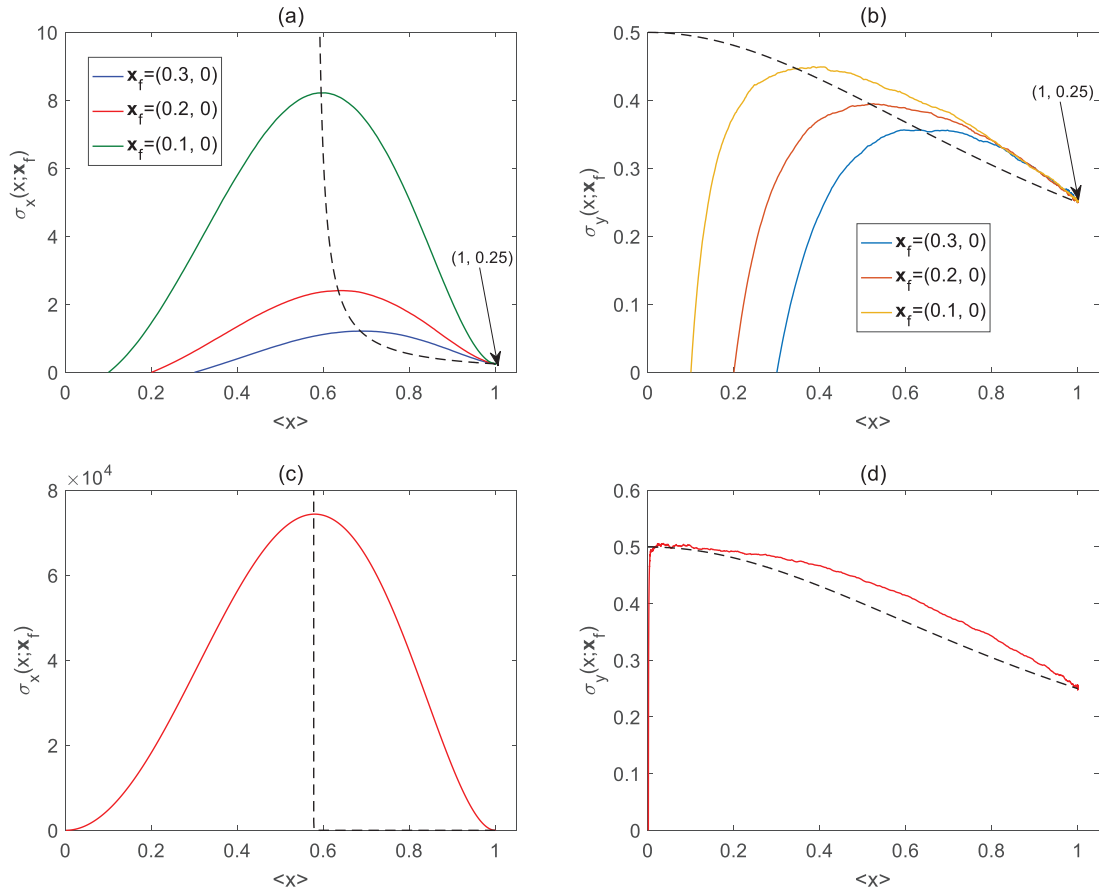
Figure 4. Dispersions for different final positions for $\alpha = \mu = 1$. (a) and (b) $\boldsymbol{x}_f = (0.3, 0)$, $(0.2, 0)$, $(0.1, 0)$; the noise strength for them is $D = 10^{-6}$. (c) and (d) $\boldsymbol{x}_f = (0.001, 0)$, the noise strength is $D = 10^{-9}$. The black dashed lines in the figures are theoretical extremal positions of the dispersion: equations (8) and (9).

$$\boldsymbol{F}\left(\boldsymbol{x}\right) = -\frac{1}{2}\nabla\psi\left(\boldsymbol{x}\right) + l\left(\boldsymbol{x}\right) \tag{11}$$

where $\nabla\psi\left(\boldsymbol{x}\right)$ is the gradient of the quasipotential and $l\left(\boldsymbol{x}\right)$ represents the rotational component, the vector field $\boldsymbol{G}\left(\boldsymbol{x}\right) = \boldsymbol{F}\left(\boldsymbol{x}\right) + \nabla\psi\left(\boldsymbol{x}\right)$ gives out the MPEP [13]. The reverse of the vector field $\boldsymbol{G}\left(\boldsymbol{x}\right)$, which we denote as $-$VG, could serve as the vector field for the relaxation simulation of the dispersion for non-gradient systems. Thus we name the method VG relaxation method.

Therefore, the method goes as: first, compute the quasipotential and its gradient $\nabla\psi\left(\boldsymbol{x}\right)$. Second, calculate the vector field $\boldsymbol{G}\left(\boldsymbol{x}\right)$ and its reverse $-$VG. Finally, start the samples from the final point and obtain the sampling paths. The dispersion can be calculated via the sampling paths.

3.2.2. The calculation of quasipotential. Therefore, the core problem would be the calculation of the quasipotential. In this paper, we apply the ordered line integral methods (OLIMs) [14] proposed by Dahiya and Cameron to compute the quasipotential. The quasipotential of system (1) for $\alpha = 6.67$, $\mu = 2$ are shown in figure 5. The starting
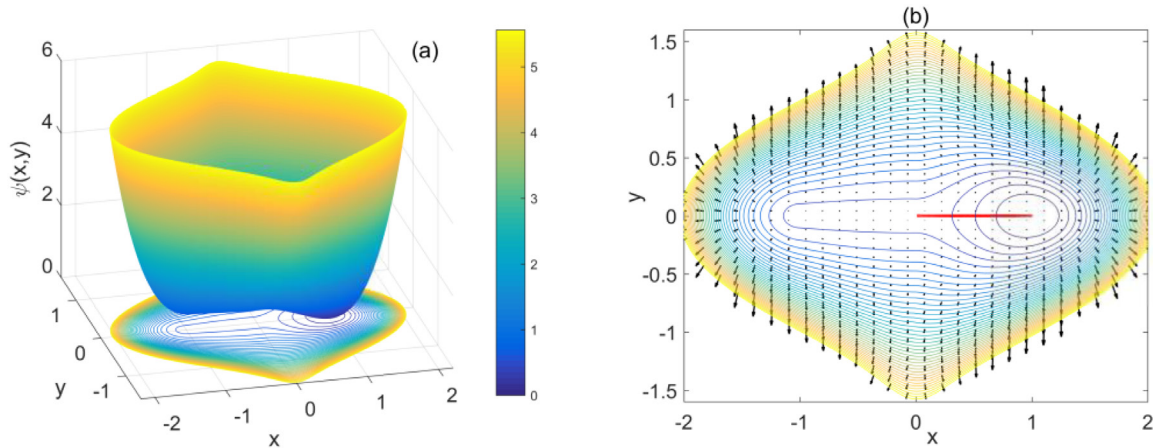
Figure 5. (a) The 3D plot and contour plot of the quasipotential of system (1). Parameters are: $\alpha = 6.67$, $\mu = 2$. The mesh is 2048×2048 with update factor $K = 26$. (b) The black arrows represent the vector field $\boldsymbol{G}(\boldsymbol{x})$ and the red line denotes the MPEP computed by shooting a flow line of the vector field $-\boldsymbol{G}(\boldsymbol{x})$ from the final point $\boldsymbol{x}_f = (0,\, 0)$.

point of OLIMs program is selected as $(1, 0)$ which accounts for the asymmetry of the landscape.

3.2.3. Case test. With the result of quasipotential, the vector field $-$VG can be easily computed. This vector field will be used as the revised relaxation method (denoted as VG relaxation method) for the dispersion of the non-gradient system. To verify the feasibility of this method, we test it for noise strength $D = 0.1$ and $\boldsymbol{x}_f = (0.4,\, 0)$. For comparison, we will denote the application of the vector field $-\boldsymbol{F}(\boldsymbol{x})$ as the old relaxation method. The results of the dispersions are shown in figure 6. From figure 6(a) we can see that the dispersion $\sigma_x(x; \boldsymbol{x}_f)$ via VG relaxation method is close to the result via old relaxation method and Monte Carlo simulation. It could be explained by the symmetry of the vector field in system (1), where the vector field along the MPEP parallels to the x-axis. For $\sigma_y(x; \boldsymbol{x}_f)$, the result of the old relaxation method has a significant difference from the Monte Carlo simulation. In contrast, the dispersion obtained by VG relaxation method agrees relatively well with the numerical results. This is because the vector field for the optimal fluctuational paths near the MPEP differs severely from the deterministic vector field. Thus, the dynamical behaviors transverse to the MPEP will have different properties between the fluctuational and relaxational processes.

One may observe that the results by VG relaxation method still have some errors compared with those of the Monte Carlo simulation. There could be two ways to reduce the errors. First, the influence of the noise strength considered in this case cannot be ignored. The application of quasipotential for weak noise situation will be more favorable. Second, the size of the mesh grid for computing the quasipotential will affect the precision of its gradient, thus the vector field $-$VG. The refinement of the mesh will make the result by VG relaxation method more accurate. The former is more dominant in the errors, and the results are more accurate by reducing the noise strength.

For different final positions, the dispersions are studied by VG relaxation method as in figure 7. The tendency of the dispersion curves show a similar behavior as the
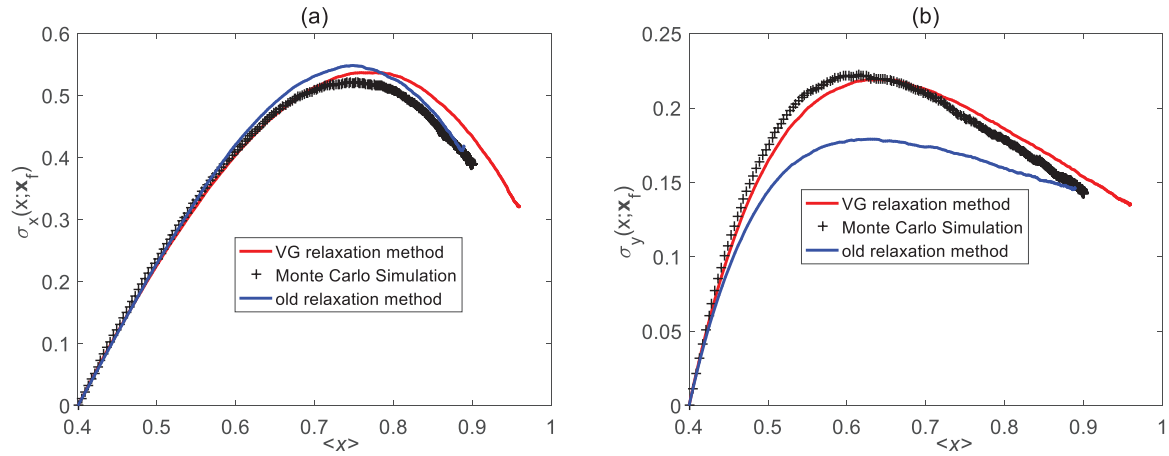
Figure 6. Comparison of the results of the dispersions between VG relaxation method and old relaxation method. (a) Dispersion along the x-direction; (b) dispersion along the y-direction. The noise strength $D = 0.1$ and the final point $\boldsymbol{x}_f = (0.4, 0)$.
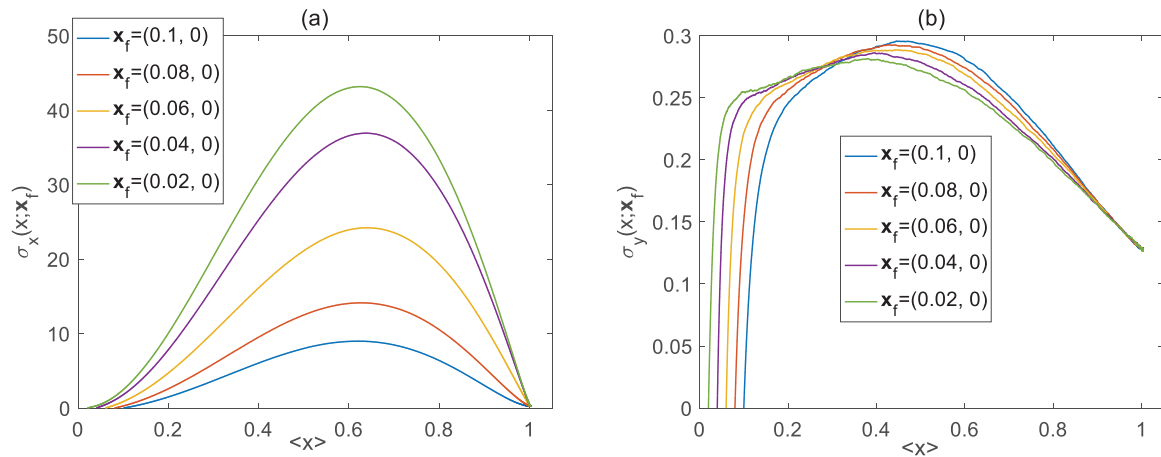

Figure 7. Dispersions for different final positions for $\alpha = 6.67$ $\mu = 2$. $\boldsymbol{x}_f = (0.1, 0)$, $(0.08, 0)$, $(0.06, 0)$, $(0.04, 0)$ and $(0.02, 0)$, the noise strength $D = 10^{-3}$. (a) Dispersion along the x-direction; (b) dispersion along the y-direction.

previous case, wherein the peak of the dispersion for both $\sigma_x(x; \boldsymbol{x}_f)$ and $\sigma_y(x; \boldsymbol{x}_f)$ gradually shifts left. The initial dispersion for $\sigma_x(x; \boldsymbol{x}_f)$ is $\sigma_x(x = 1; \boldsymbol{x}_f) \approx 0.267$ and for $\sigma_y(x; \boldsymbol{x}_f)$ is $\sigma_y(x = 1; \boldsymbol{x}_f) \approx 0.128$.

3.3. Case $\alpha = 6.67$ $\mu = 1$

For this case, the MPEP no longer follows the x-axis which is a manifestation of symmetry breaking. Two different paths have the same action value, i.e. either one is the MPEP as in figure 2(c). The quasipotential landscape and the vector field $\boldsymbol{G}(\boldsymbol{x})$ are illustrated in figure 8. To investigate the dispersion in this case, we limit the exit paths close to the upper branch (see the red curve in figure 8(b)). In this case, the relaxational path will not coincide with the fluctuational path as can be seen in figure 9. The errors between Monte Carlo simulation and VG relaxation method can be explained similarly as above.
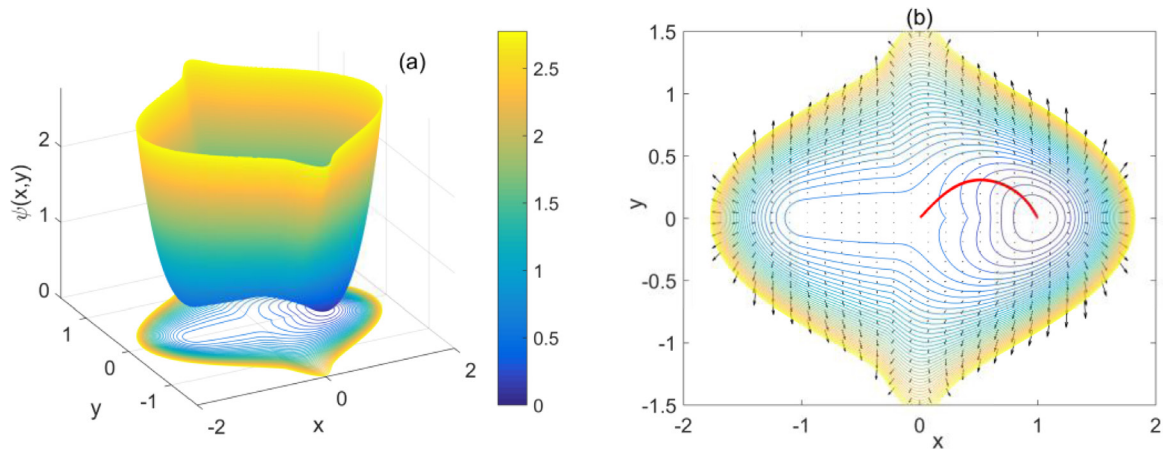
Figure 8. (a) The 3D plot and contour plot of the quasipotential of system (1). Parameters are: $\alpha = 6.67$, $\mu = 1$. The mesh is 2048×2048 with update factor $K = 26$. (b) The black arrows represent the vector field $\boldsymbol{G}(\boldsymbol{x})$ and the red curve denotes the MPEP computed by shooting a flow line of the vector field $-\boldsymbol{G}(\boldsymbol{x})$ from the final point $\boldsymbol{x}_f = (0, 0)$.
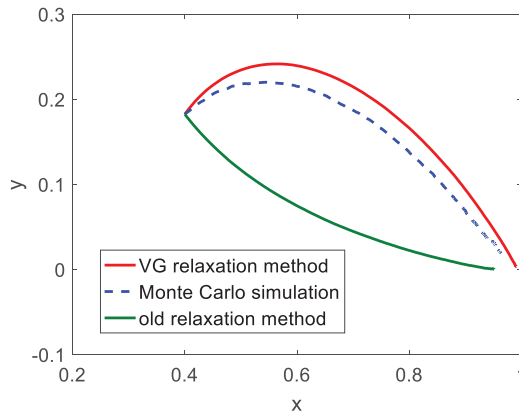

Figure 9. Averaged paths for three different methods. The final point $\boldsymbol{x}_f = (0.4, 0.1825)$. Noise strength $D = 0.03$.

The results of the dispersion via VG relaxation method and Monte Carlo simulation are shown in figure 10. The final point $\boldsymbol{x}_f = (0.4, 0.1825)$ and noise strength $D = 0.03$. The error of these two methods is within the tolerable range since the averaged paths have a visible difference as is in figure 9. The precision can be improved by reducing the noise strength and refining the mesh grid for the quasipotential.

For small noise strength $D = 10^{-4}$, the dispersions are studied via VG relaxation method. The results are shown in figure 11. The final points are selected along the MPEP illustrated in figure 8(b). For the dispersion $\sigma_x(x; \boldsymbol{x}_f)$, the peak gradually shift left for the final point approaches the saddle. The initial dispersion $\sigma_x(x = 1; \boldsymbol{x}_f) \approx 0.267$ which is the same as the previous case. Recall that the initial dispersion is related to the marginal stationary probability distribution around the stable equilibrium $(1, 0)$. Because $\alpha = 6.67$ in both cases, the marginal stationary probability distribution should be the same, which in turn makes the initial dispersion $\sigma_x(x = 1; \boldsymbol{x}_f)$ the same. For $\sigma_y(x; \boldsymbol{x}_f)$, as $\boldsymbol{x}_f$ is more close to the saddle point, two peaks will emerge and the valley
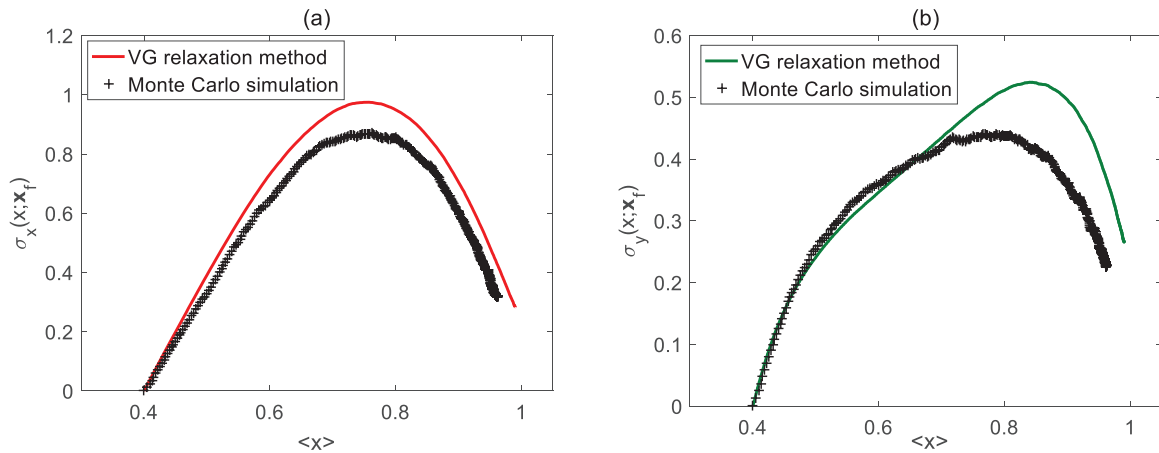
Figure 10. Dispersions for VG relaxation method and Monte Carlo simulation. The noise strength $D = 0.03$ and the final point $\boldsymbol{x}_f = (0.4, 0.1825)$.
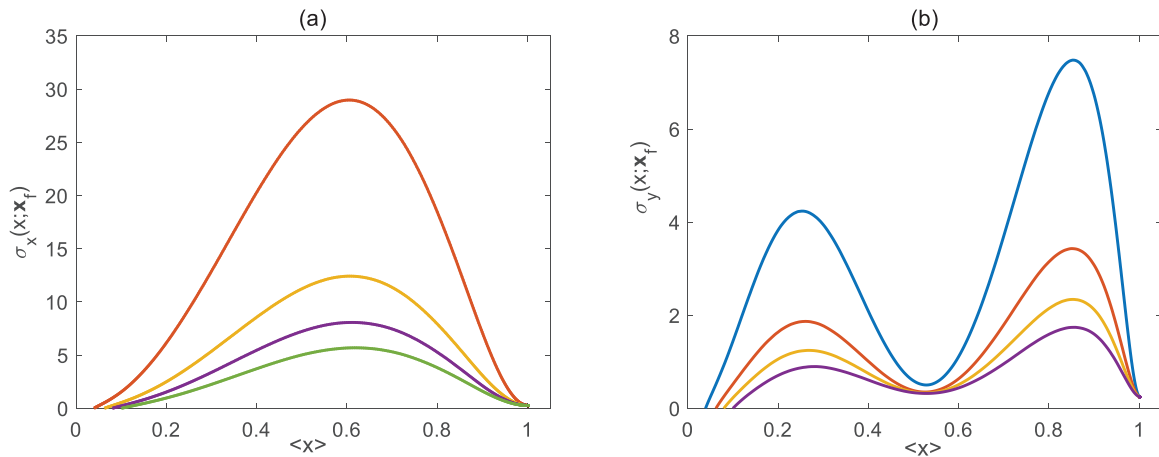

Figure 11. Dispersions for different final positions for $\alpha = 6.67$ $\mu = 1$. $\boldsymbol{x}_f = (0.039\,38, 0.041\,62)$, $(0.062\,40, 0.064\,61)$, $(0.079\,83, 0.081\,69)$ and $(0.1, 0.1)$, the noise strength $D = 10^{-4}$.

between the peaks becomes more apparent. The valley is around $\langle x \rangle \approx 0.53$ which shows nearby exit paths accumulate more tightly in this site. Thus, one can predict the exit process on this site more accurately.

4. Discussions and conclusions

The dispersions of the exit phenomena in the Maier–Stein system for three sets of parameters are studied in this paper. For the gradient case, the dispersion is computed via the traditional relaxation method extended to the 2D situation. For the non-gradient case, a revised version of the relaxation method is proposed which involves the calculation of the quasipotential of the system (the quasipotential is also called the rate function in statistical mechanics [31]). The results of the two relaxation methods are compared with those of Monte Carlo simulation, which show a relatively good agreement. In all those cases, the dispersion shows a non-monotonic behavior during the

exit process. Moreover, the initial dispersion keeps constant as the final point changes. This can be explained that the initial dispersion is related to the stationary probability distribution around the stable equilibrium. It should be noted that in Case 2, because of the symmetry of the system, the MPEP follows the time-reversed path of the relaxation in spite of the breaking of the time-reversal symmetry. However, the dispersion can be wrong if it is computed via traditional relaxation method, which is caused by the changed fluctuation behaviors near the MPEP. It should be noted that the method described in this paper is applicable to other non-gradient systems without detailed balance.

The MPEP determines the most probable behavior for vanishing noise. While for finite noise strength in real physical systems, the sampling paths will not completely follow the MPEP. The dispersion during the exit process reveals the sensitivity of the paths near the MPEP. The smaller the dispersion, the more accurate for an observer to determine exit location.

The proposed algorithm is an initial attempt in computing the dispersion in non-gradient systems. The accuracy depends largely on the calculation of the quasipotential, which is still a difficult task for high-dimensional systems. With the fast development of the computer science, it can be inferred that our algorithm can be extended to high-dimensional systems.

Acknowledgments

References

[1] David L and Luis B 2010 Urban noise and the cultural evolution of bird songs *Proc. R. Soc.* B **277** 469–73
[2] Deco G, Jirsa V, McIntosh A R, Sporns O and Kotter R 2009 Key role of coupling, delay, and noise in resting brain fluctuations *Proc. Natl Acad. Sci.* **106** 10302–7
[3] Zhu L and Wang Y 2017 Rumor spreading model with noise interference in complex social networks *Physica A* **469** 750–60
[4] Cerulus B, New A M, Pougach K and Verstrepen K J 2016 Noise and epigenetic inheritance of single-cell division times influence population fitness *Curr. Biol.* **26** 1138–47
[5] Gammaitoni L, Hänggi P, Jung P and Marchesoni F 1998 Stochastic resonance *Rev. Mod. Phys.* **70** 223–87
[6] Pikovsky A S and Kurths J 1997 Coherence resonance in a noise-driven excitable system *Phys. Rev. Lett.* **78** 775–8
[7] Freidlin M I and Wentzell A D 2012 *Random Perturbations of Dynamical Systems* (Berlin: Springer)
[8] De La Cruz R, Perez-Carrasco R, Guerrero P, Alarcon T and Page K M 2018 Minimum action path theory reveals the details of stochastic transitions out of oscillatory states *Phys. Rev. Lett.* **120** 128102
[9] Qiao L, Zheng Z and Cross M C 2016 Minimum-action paths for wave-number selection in nonequilibrium systems *Phys. Rev.* E **93** 042204
[10] Chen X, Wu F, Duan J, Kurths J and Li X 2019 Most probable dynamics of a genetic regulatory network under stable Lévy noise *Appl. Math. Comput.* **348** 425–36
[11] Heymann M and Vanden-Eijnden E 2008 The geometric minimum action method: a least action principle on the space of curves *Commun. Pure Appl. Math.* **61** 1052–117
[12] Beri S, Mannella R, Luchinsky D G, Silchenko A N and McClintock P V E 2005 Solution of the boundary value problem for optimal escape in continuous stochastic systems and maps *Phys. Rev.* E **72** 036131

[13] Cameron M K 2012 Finding the quasipotential for nongradient SDEs *Physica* D **241** 1532–50

[14] Dahiya D and Cameron M 2018 Ordered line integral methods for computing the quasi-potential *J. Sci. Comput.* **75** 1351–84

[15] Dahiya D and Cameron M K 2018 An ordered line integral method for computing the quasi-potential in the case of variable anisotropic diffusion *Physica* D **382–3** 33–45

[16] Yang S, Potter S F and Cameron M K 2019 Computing the quasipotential for nongradient SDEs in 3D *J. Comput. Phys.* **379** 325–50

[17] Dykman M I, McClintock P V E, Smelyanski V N, Stein N D and Stocks N G 1992 Optimal paths and the prehistory problem for large fluctuations in noise-driven systems *Phys. Rev. Lett.* **68** 2718–21

[18] Luchinsky D G, Maier R S, Mannella R, McClintock P V E and Stein D L 1999 Observation of saddle-point avoidance in noise-induced escape *Phys. Rev. Lett.* **82** 1806

[19] Morillo M, Casado J M and Gómez-Ordóñez J 1997 Brownian dynamics simulation of the prehistory problem *Phys. Rev.* E **55** 1521

[20] Arrayás M, Casado J M, Ordóñez J G, McClintock P V E, Morillo M and Stein N D 1998 Dispersion of the prehistory distribution: analog experiments and numerical results *Phys. Rev. Lett.* **80** 2273

[21] Luchinsky D G and McClintock P V E 1997 Irreversibility of classical fluctuations studied in analogue electrical circuits *Nature* **389** 463–6

[22] Piñeiro Orioli A and Berges J 2019 Breaking the fluctuation-dissipation relation by universal transport processes *Phys. Rev. Lett.* **122** 150401

[23] Maier R S and Stein D L 1993 Escape problem for irreversible systems *Phys. Rev.* E **48** 931–8

[24] Maier R S and Stein D L 1997 Limiting exit location distributions in the stochastic exit problem *SIAM J. Appl. Math.* **57** 752–90

[25] Luchinsky D G, Maier R S, Mannella R, McClintock P V E and Stein D L 1997 Experiments on critical phenomena in a noisy exit problem *Phys. Rev. Lett.* **79** 3109–12

[26] Maier R S and Stein D L 1996 A scaling theory of bifurcations in the symmetric weak-noise escape problem *J. Stat. Phys.* **83** 291–357

[27] Maier R S and Stein D L 1993 Effect of focusing and caustics on exit phenomena in systems lacking detailed balance *Phys. Rev. Lett.* **71** 1783–6

[28] Crooks G E and Chandler D 2001 Efficient transition path sampling for nonequilibrium stochastic dynamics *Phys. Rev.* E **64** 026109

[29] Chen Z and Liu X 2017 Singularities of fluctuational paths for an overdamped two-well system driven by white noise *Physica* A **469** 206–15

[30] Zhu J, Chen Z and Liu X 2018 Probability evolution method for exit location distribution *Phys. Lett.* A **382** 771–5

[31] Touchette H 2009 The large deviation approach to statistical mechanics *Phys. Rep.* **478** 1–69